A DECISION TREE FOR INFLIGHT DATA PROCESSING FOR ROBOT SPACECRAFT TRAJECTORY GUIDANCE

A.M. Chande'

SASC Technologies Inc.
Scientific Systems Division
4400 Forbes Blvd.
Lanham, MD. 20706

R.W. Newcomb

University of Maryland
Microsystems Lab
Electrical Engineerings Dept.
College Park, MD. 20742

Abstract

This paper gives a decision tree for processing on-board sensory data to aid autonomous trajectory determination for a robotic space vehicular system.

The wealth of sensory data obtained from spacecraft automated sensors and multisource correlators forms the data segment of the data base. Decision making for these systems is aided by top-down AND/OR back-trackable tree searches and heuristics which are ideal for coding in a computationally intensive programming language. A strategy for autonomous trajectory determination and execution will enable space vehicles to be safe and smart.

The Contemporary Modus Operandi

The capabilities of current on-board spacecraft processors have been pushed to their limits, and the decision making is primarily carried out at ground-based mission controls via electro-magnetic wave umbilicals that transport crucial information. Time that is critical to the decision making process is lost in delays in terms of modulation and transmission channel throughputs. This can be significant for large distances in space. Further, the on-board processor bytes have to accomodate error-detecting and error-correcting codes to be able to achieve a high information channel reliability in addition to accommodating encryption bits for link security for protection from malicious interferences[1]. The processor may have a software overhead associated with formatting and deformatting transponder headers and decryption routines. NASA software specialists recommend that "the flight software should be designed to permit in-orbit programming to enhance operations or work around equipment failures[2]."

Automation

To be able to overcome such problems, we recommend the incorporation of highly correlated automated sensors with a computationally intensive expert system aid to roboticize the spacecraft. This paper conceptually outlines an advanced robotic space vehicular system; Figure 1. The automated sensor domain and the expert processor domain have been demarcated. The sensors are, typically, transducers with digital outputs that can be sent over a common processor bus interfaced by multiplexers, as is done on present-day spacecraft. The wealth of sensory data from the boosters, main engine, aerosurface actuators, inertial measurement units and infra-red detectors is disseminated and correlated into a sensory input vector that feeds the dynamic knowledge base. The input vector $\overrightarrow{NR}$ is augmented with navigation aid parameters and space geometry parameters to comprise the navigation resources that are constantly updated by the information maintenance section of the dynamic knowledge base. The knowledge base also has prestored heuristic production rules. The inference engine is essentially a static mechanism invoked by the rule driven knowledge base at appropriate stages in the trajectory; Figure 2. The Expert Event Scheduler Executive (EESE) makes and justifies conclusions by first analyzing the sensory data and then event profiling in terms of production rule primitive subgoals. The trajectory determination decisions are viable goals given subgoal conglomerates. The goal states can be used for trajectory navigation unless aborted by overriding signals from the dynamic automated sensors or correlating instrumentation.

The EESE inference engine can be constructed in many ways. Strategies for decomposable production systems utilizing theorem-proving systems can be realized with top-down searches of AND-OR trees[3]. A trajectory determination AND/OR tree is depicted in Figure 3. The expert system can be configured from already existing navigation and space geometry routines in FORTRAN by a semantic mechanism that knits the component programs together for real-time processing. LISP has a slow processor run cycle time and can be embarrassing for real-time decision making. Typical run-time operations for resolution of 50-200 horn clauses on a VAX 11/780 using Franz-LISP is around 0.5 seconds[4]. There is no demonstrable evidence that one computer language is greatly superior to another, however the processing speed is an important criteria for real-time applicability. Since translations of FORTRAN to LISP, LISP to FORTRAN, and LISP to Ada are being currently marketed by Systems Research Labs, many software experts believe that they can code such a task in any reasonably good language. It is our contention that the language of implementation is relatively unimportant in this specific application domain and that though it should be a higher order language , Ada or FORTRAN will most certainly do the job, based on their rapid processing capabilities and computation

intensiveness.

The objective of automating the space vehicle is to lessen the burden caused by the repetitive surveillance and monitoring tasks carried out at earth mission controls. It would also result in timely planning of obvious trajectories and increase mission survivability in hostile space environments.

The global sequence for spacecraft maneuvers has been presented in concatenated stages from launch to land, whether it is with reference to the earth or any other planet. The EESE will be constantly cognizant of these stages and their immediate neighbor stages during the event profiling for autonomous navigation and trajectory selection.

Trajectory calculations for Figure 3 are aptly suited for a computationally intensive language for permissible orbital maneuvers under the two, three or more than three-body problem conditions. After the trajectory is calculated, stability calculations must be performed before the predicted path can be navigated; this has been shown by the AND connective. The previous and next stage situation determines the value of n in the n body problem, and heuristics further determine allowable trajectories or backtracking routes.

Figure 4 shows the feasibility of integrating already existing shuttle avionics software (PASS) and the EESE to yield next-generation software capable of rendering the spacecraft autonomous. This autonomy will not be absolute since the crew could be considered as a hot stand-by (human) redundancy; as quoted in[5] "the human component provides a lot of flexibility for problem solving."

Any changes in critical astrodynamical and astronic parameters would necessitate orbital motion planning and the need to determine perturbed orbital stability and sensitivity in real time. For the spacecraft to be able to execute the replanned trajectory, in-orbit attitude maneuvers would have to be sequenced. This not only would require the examination of momentum precession and adjustment for rigid spacecraft for both constant and rigid bias applications, but it would also require the prediction of corresponding strategies for vehicular detumbling and inclination control by yaw sensing. Calculations for interplanetary transfers, trajectory planning between two points, and relative motion of neighboring-orbit bodies is examined via the decision tree for every trajectory planned. For every stage x_i of the global maneuver sequence, a corresponding top-down search of the trajectory tree can be made for a 2-body, 3-body or n-body problem. During transitions of stages x_1 through x_{17}, the number of bodies in context may change and a suitable backtracking algorithm can accomodate appropriate trajectory searches in such cases. Most likely trajectories for the 2 and 3-body problem are depicted in Figure 5.

Appendix I Trajectory Calculations

Here we discuss the pertinent transfers for spacecraft in the 2-body problem[6] under the search tree. The transfers for spacecraft that change between two consecutive stages labelled x_1 through x_{17} are as follows:

(i) Orbit transfer at apogee,
(ii) Hohman transfer,
(iii) Coplaner transfer,
(iv) Orbital plane rotation transfer,
(v) Planetary capture.

The associated conic sections representing the most likely orbited trajectories are represented in Figure 5. Given polar coordinates (r, θ), (r, ϕ), the angular momentum h and the gravitational constant μ, the radius r is

$$r = \frac{h^2}{\mu} \Big/ \left(1 + e \cos \theta \right) \qquad ...(1)$$

and the eccentric anomally is given by

$$\cos \psi = \frac{a e + r \cos \theta}{a} \qquad ...(2)$$

where e is the eccentricity. A single thrust impulse applied a point in the orbital plane can cause the orbit transfer and for a known r the changed speed at transfer is given by

$$v = \left[\frac{2\mu}{r} - \frac{\mu}{a} \right]^{1/2} \qquad ...(3)$$

and at the apogee by

$$v = \left[\frac{\mu}{a} \left(\frac{1 - e}{1 + e} \right) \right]^{1/2} \qquad ...(4)$$

An orbital transfer between two circular cocentric orbits is termed as Hohman transfer and the minimum escape velocity is

$$\Delta v = \left(\sqrt{2} - 1 \right) \left[\frac{\mu}{r_i} \right]^{1/2} \qquad ...(5)$$

for an outer to inner orbit radius ratio of $\frac{r_o}{r_i} = 3.4$

Coplaner orbit transfers between coaxial elliptic orbits of eccentricity e_i and e_o requires a periapsial impulse of

$$\Delta v_i = \left[\frac{\mu}{r_i} \left\{ \frac{2 \left(r_o / r_i \right)}{1 + \left(r_o / r_i \right)} \right\} \right]^{1/2} - \left[\frac{\mu}{r_i} \left\{ 1 + e_i \right\} \right]^{1/2} \qquad ...(6)$$

and a second apoapsial impulse of

$$\Delta v_o = \left[\frac{\mu}{r_o} \left\{ 1 - e_o \right\} \right]^{1/2} - \left[\frac{\mu}{r_o} \left\{ \frac{2}{1 + \left(r_o / r_i \right)} \right\} \right]^{1/2} \qquad ...(7)$$

In a plane rotation transfer the change in velocity is the old velocity times the change in the angle of precession of the angular momentum vector.

A planetary capture for missions terminating in an orbit around planet z, a minimum velocity delta is achieved when

$$r_z = \frac{2\mu_z}{v_{\infty/z}^2} \qquad ...(8)$$

where v_∞ is the relative velocity at a large distance of r.

The 3-body problem may require other transfers such as

those detailed below:

(i) Hyperbolic interplanetary transfer,
(ii) Heliocentric transfer,
(iii) Lunar transfer,
(iv) Planetary capture.

The interplanetary transfers are achieved by the patched conics method and a hyperbolic passage is necessary.

A heliocentric orbit around other planets requires a hyperbolic escape path and the velocity at perigee must be adjusted.

Lunar transfers are normally designed as free-return trajectories, so that safe return to the earth is possible without rocket power.

Planetary capture is accomplished by a decelerating impulse that reduces energy of the hyperbolic ingress passage.

Appendix II Orbit Geometry and Stability Calculations

This appendix details the computational implications of trajectory calculations and attitude control calculations.

The frames of reference, shown in Figure 6 are the inertial frame of reference (X,Y,Z) and the body fixed frame of reference (x,y,z). The Euler's angles uniquely determine the body orientation in terms of the orthogonal transformation property of

$$\sum \alpha_{ij}\ \alpha_{ik} = \delta_{jk} \qquad \forall\ j,k = 1,2,3 \qquad ...(9)$$

Figure 5 depicts the Euler's angles construction by

(i) Rot (Z, ψ) to yield a new (Z',Y',X') axes
(ii) Rot (X', θ) to yield a new (Z",Y",X") axes
(iii) Rot (Z", ϕ) to yield the body's (x,y,z) axes.

The direct transformation between (x,y,z) and (X,Y,Z) can be represented by

$$\begin{bmatrix} x \\ y \\ z \end{bmatrix} = \alpha\beta\gamma \begin{bmatrix} X \\ Y \\ Z \end{bmatrix} \qquad ...(10)$$

where

$$\alpha = \begin{bmatrix} \cos\phi & \sin\phi & 0 \\ -\sin\phi & \cos\phi & 0 \\ 0 & 0 & 1 \end{bmatrix} \qquad ...(11)$$

$$\beta = \begin{bmatrix} 1 & 0 & 0 \\ 0 & \cos\theta & \sin\theta \\ 0 & -\sin\theta & \cos\theta \end{bmatrix} \qquad ...(12)$$

$$\gamma = \begin{bmatrix} \cos\psi & \sin\psi & 0 \\ -\sin\psi & \cos\psi & 0 \\ 0 & 0 & 1 \end{bmatrix} \qquad ...(13)$$

Further, the angular velocity vector ω can be expressed in terms of the rates of change of Euler's angles

$$\begin{bmatrix} \omega_x \\ \omega_y \\ \omega_z \end{bmatrix} = \begin{bmatrix} \sin\theta\sin\phi & \cos\phi & 0 \\ \sin\theta\cos\phi & -\sin\phi & 0 \\ \cos\theta & 0 & 1 \end{bmatrix} \begin{bmatrix} \dot{\psi} \\ \dot{\theta} \\ \dot{\phi} \end{bmatrix} \qquad ...(14)$$

From which the rates of change of Euler's angles can be written as

$$\begin{bmatrix} \dot{\psi} \\ \dot{\theta} \\ \dot{\phi} \end{bmatrix} = \frac{1}{\sin\theta} \begin{bmatrix} \sin\phi & \cos\phi & 0 \\ \cos\phi\sin\theta & -\sin\phi\sin\theta & 0 \\ -\sin\phi\cos\theta & -\cos\phi\cos\theta & \sin\theta \end{bmatrix} \begin{bmatrix} \omega_x \\ \omega_y \\ \omega_z \end{bmatrix} \qquad ...(15)$$

In the two body problem, the rotation about the center of mass under the influence of applied torques is termed as attitude dynamics for the spacecraft. The moment of momentum h_o , is given in terms of the moments of inertia and the angular velocity vector as

$$h_o = \begin{bmatrix} h_x \\ h_y \\ h_z \end{bmatrix} = \begin{bmatrix} I_x & -I_{xy} & -I_{xz} \\ -I_{xy} & I_y & -I_{yz} \\ -I_{xz} & -I_{yz} & I_z \end{bmatrix} \begin{bmatrix} \omega_x \\ \omega_y \\ \omega_z \end{bmatrix} \qquad ...(16)$$

For torque-free motion of asymmetrical bodies, Euler's moment equations are given in terms of DEs relating applied torgue components to angular momentum changes.

$$\begin{aligned} M_x &= \dot{h}_x + \omega_y h_z - \omega_z h_y \\ M_y &= \dot{h}_y + \omega_z h_x - \omega_x h_z \\ M_z &= \dot{h}_z + \omega_x h_y - \omega_y h_x \end{aligned} \qquad ...(17)$$

The orientation with respect to an inertial direction is termed as the rotation angle θ_n and the precession rate is given by

$$\dot{\psi} = \frac{I_3\,\dot{\phi}}{(I_1 - I_3)\cos\theta_n} \qquad ...(18)$$

which is a constant and if $\dot{\psi}$ and $\dot{\phi}$ are in opposite directions it is termed as retrograde precession whereas if $\dot{\psi}$ and $\dot{\phi}$ are undirectional than the precession is direct. This type of motion is described by using motion cones.

For stability of torque free motion λ must be real and is given by

$$\lambda = \sqrt{\frac{(I_1 - I_2)(I_1 - I_3)}{I_2 I_3}\,\omega_o^2} \qquad ...(19)$$

If λ is imaginary then ω_i will diverge and the motion is unstable.

References

1. E. Fthenakis, Manual of Satellite Communications, McGraw-Hill Book Company, N.Y.,1984, 351 pages.

2. C. E. Trevathan, T. D. Taylor, R. G. Hartenstein, A. C. Merwarth, and W. N. Stewart, "Development and Application of NASA's First Standard Spacecraft Computer," Communications of the ACM, September 1984, Vol 27, Number 9, pp. 902-913.

3. N. J. Nilsson, Principles of Artificial Intelligence, Tioga Publishing Company, 1980, 476 pages.

4. K. Niwa, K. Sasaki, H. Ihara, "An Experimental Comparison of Knowledge Representation Schemes," The AI Magazine, Summer 1984, Vol.5,pp. 29-36.

5. A. Spector and D. Gifford, "The Space Shuttle Primary Computer System," Communications of the ACM, September 1984, Vol. 27, Number 9, pp. 875-900.

6. M. H. Kaplan, Modern Spacecraft Dynamics & Control, John Wiley & Sons, N.Y., 1976, 415 pages.

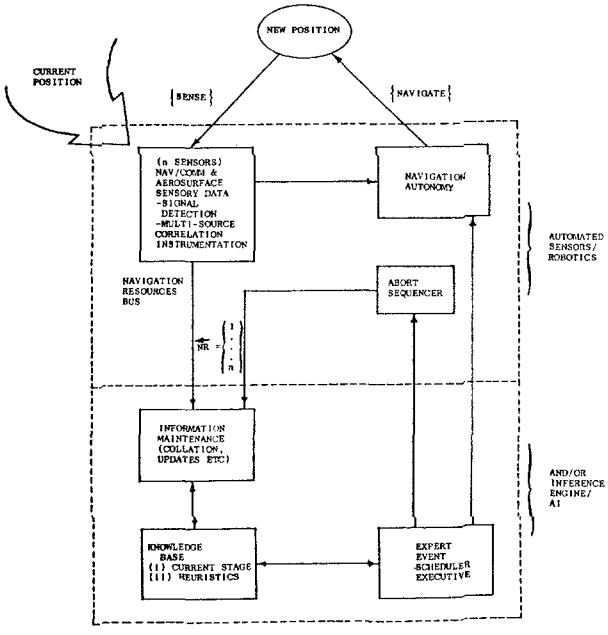

Figure 1. Information System for an Advanced Robotic Space Vehicular System.

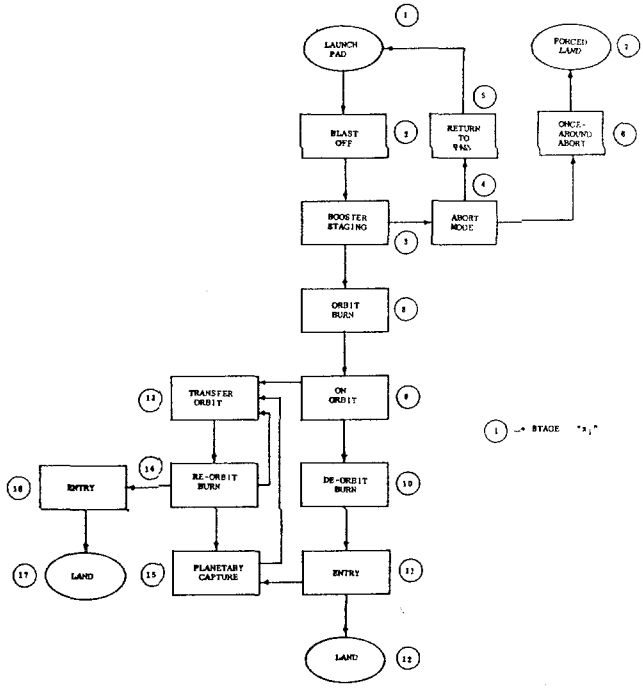

Figure 2. Sequence Stages for Spacecraft Maneuvers.

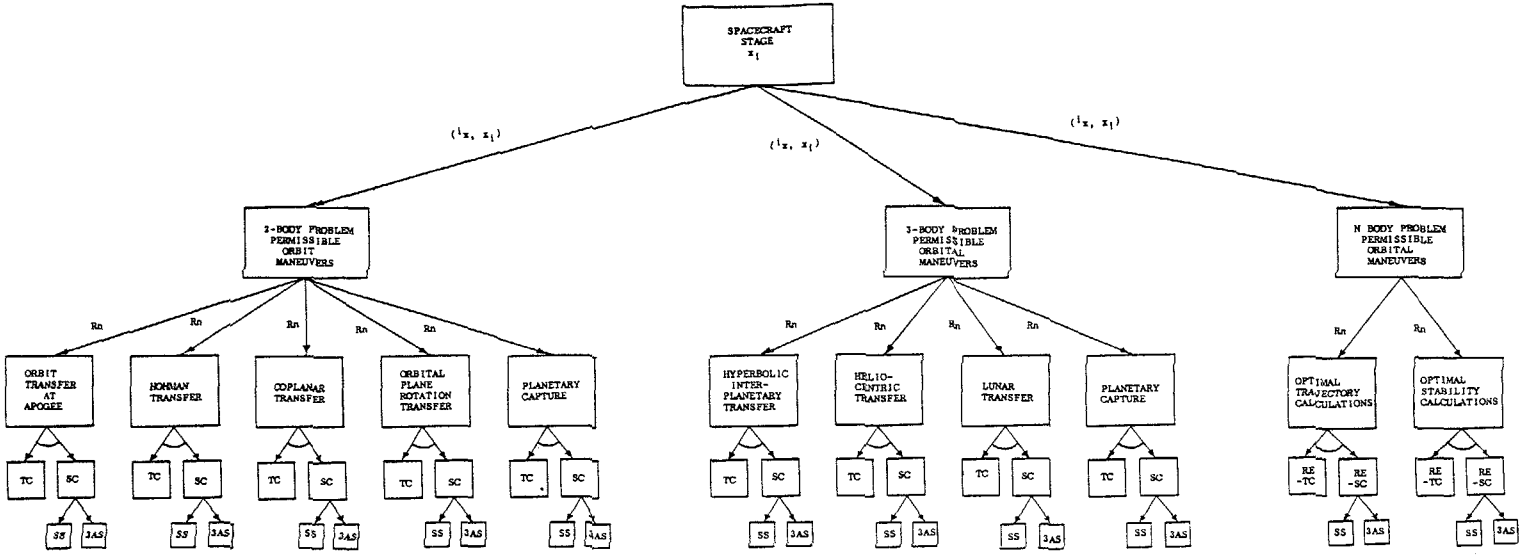

- OR CONNECTIVE
- AND CONNECTIVE
$(^1x, x_i)$ - (STAGE PREVIOUS TO x_i, STAGE SUBSEQUENT TO x_i)
i - STAGE 1 THROUGH 17
Rn - HEURISTIC n

TC = TRAJECTORY CALCULATIONS
SC = STABILITY CALCULATIONS/ ATTITUDE DYNAMICS
SS = SPIN STABILIZATION
3AS = 3 AXIS STABILIZATION

Figure 3. Trajectory Search Graph.

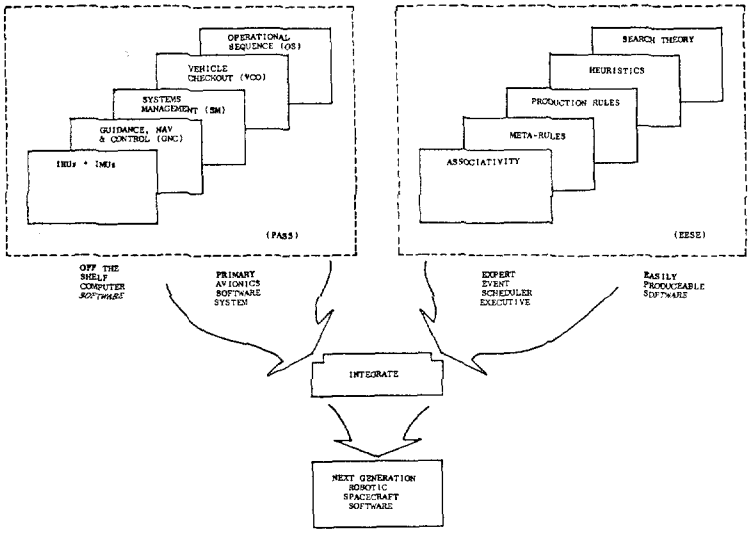

Figure 4. Smart Software.

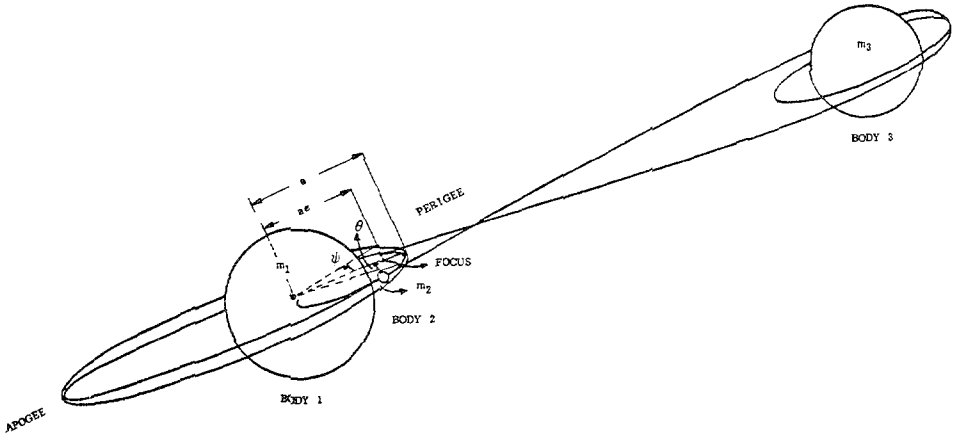

Figure 5. Three Bodies and Permissible Trajectories.

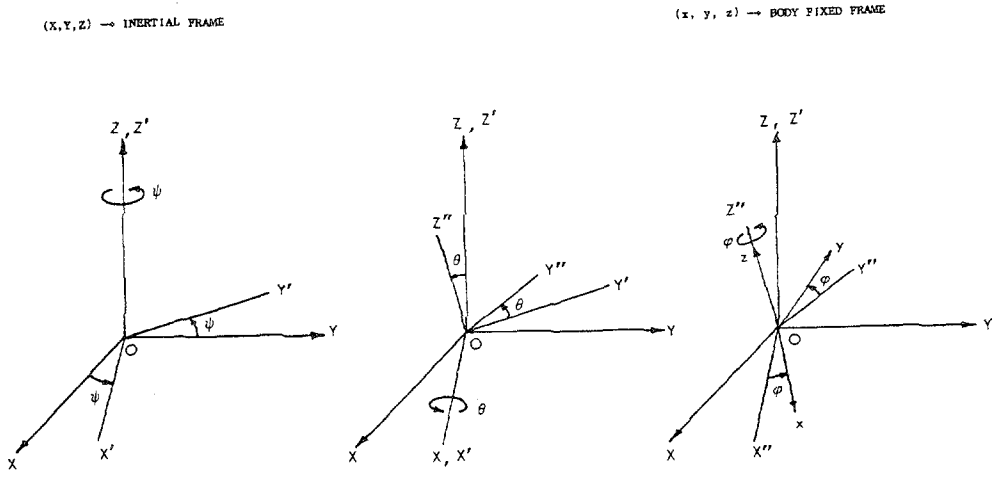

Figure 6. Frames of Reference.